THE JOURNAL OF BIOLOGICAL CHEMISTRY VOL. 283, NO. 49, pp. 33858–33864, December 5, 2008

FLN29 Deficiency Reveals Its Negative Regulatory Role in the Toll-like Receptor (TLR) and Retinoic Acid-inducible Gene I (RIG-I)-like Helicase Signaling Pathway*

Received for publication, September 8, 2008 Published, JBC Papers in Press, October 10, 2008, DOI 10.1074/jbc.M806923200

Takahito Sanada[‡], Giichi Takaesu[‡], Ryuichi Mashima[§], Ryoko Yoshida[‡], Takashi Kobayashi[‡], and Akihiko Yoshimura[‡¶‖1]

From the [‡]Division of Molecular and Cellular Immunology, Medical Institute of Bioregulation, Kyushu University, Fukuoka 812-8582, Japan, the [§]Division of Genetics, The Institute of Medical Science, The University of Tokyo, Tokyo 108-8639, Japan, the [¶]Department of Microbiology and Immunology, Keio University School of Medicine, Tokyo 160-8582, Japan, and [‖]CREST, Japan Science and Technology Corporation, Kawaguchi 332-001, Japan

***FLN29* was identified as an interferon (IFN)-inducible gene, and it has been shown to suppress Toll-like receptor 4-mediated NF-κB activation by binding to TRAF6. To elucidate the physiological roles of FLN29, we generated FLN29-deficient mice. FLN29 deficiency resulted in hyper-response to LPS both *in vivo* and *in vitro*, demonstrating the negative regulatory role of FLN29 in TLR4 signaling. Furthermore, we found that FLN29$^{-/-}$ mice exhibited increased susceptibility to poly(I:C)-induced septic shock compared with WT mice. FLN29$^{-/-}$ fibroblasts were highly resistant to vesicular stomatitis virus infection, and these cells produced more IFN-β than WT cells did in response to not only intracellular poly(I:C) but also overexpression of IPS-1. Forced expression of FLN29 inhibited the IPS-1-dependent activation of both NF-κB and IRF3. We also found that FLN29 could interact with TRIF, IPS-1, TRAF3, and TRAF6. Together, these results suggest that FLN29, in addition to playing a negative regulatory role in the TLR4 signaling pathway, negatively regulates the RIG-I-like helicase signaling pathway at the level of IPS-1/TRAF6 and IPS-1/TRAF3 complexes.**

The innate immune system is an important mechanism that confers host defense against viral and microbial infection. Three classes of pattern recognition receptors have been identified, namely Toll-like receptors (TLRs),[2] retinoic acid-inducible gene I (RIG-I)-like helicases (RLHs), and nucleotide-binding oligomerization domain (NOD)-like receptors (NLRs) (1). These receptors recognize molecular patterns specific to microorganisms, leading to the induction of inflammatory cytokines and type I interferons (IFNs).

TLRs recognize bacterial components such as lipopolysaccharide (LPS), peptidoglycan, flagellin, and CpG-DNA, as well as viral single-stranded RNA (ssRNA) and double-stranded RNA (dsRNA). TLR-dependent gene expression is induced through the activation of two distinct signaling pathways mediated by the Toll/IL-1 receptor (TIR) domain-containing adapters, called MyD88 and TRIF. These signaling pathways eventually culminate in the activation of several transcription factors, including AP-1, nuclear factor-κB (NF-κB), and interferon regulatory factor (IRF) families (2).

RLHs, such as RIG-I and melanoma differentiation antigen 5 (MDA5), were identified as sensors of cytoplasmic viral dsRNA (3, 4). RLHs, upon recognition of viral dsRNA, recruit an adapter protein called IFN-β promoter stimulator-1 (IPS-1) (also known as Cardif, MAVS and VISA) through the homotypic interactions of CARD domains, and activate downstream signaling pathways (5–8). Once activated, IPS-1 most likely serves as a platform for the assembly of downstream signaling molecules such as TRAF3, TRAF family member-associated NF-κB activator (TANK), TANK-binding kinase (TBK1), and inhibitor of κB kinase ε (IKKε). Activated TBK1 and IKKε phosphorylate and activate IRF3 transcription factor (5–8). TRAF2 and TRAF6 have also been reported to interact with IPS-1, and this interaction has been implicated in the activation of NF-κB pathway (8). Activation of both IRF3 and NF-κB is essential for the optimal induction of type I IFNs in response to viral dsRNA (9, 10).

Although the inflammatory response is critical to control the growth of pathogenic microorganisms, excessive cytokine production is harmful to the host (11). Negative feedback regulators of TLR and RLH signaling are important to protect the host from excessive immune response (1). SOCS1, IRAK-M, and A20 have been identified as such negative regulators of the TLR-NF-κB pathway (12–14). Additionally, DUBA, RNF125,

* This work was supported in part by special Grants-in-Aid from the Ministry of Education, Culture, Sports, Science, and Technology of Japan, the Program for Promotion of Fundamental Studies in Health Sciences of the National Institute of Biomedical Innovation (NIBIO), the Nakatomi Foundation, the Takeda Science Foundation, The Kato Memorial Trust Foundation for Nanbyo Research, the Suzuken Memorial Foundation, the Japan Intractable Disease Research Foundation, the Mitsubishi Pharma Research Foundation, the Uehara Memorial Foundation, the Astellas Foundation for Research on Metabolic Disorders, the Yakult Bioscience Research Foundation, and the Princess Takamatsu Cancer Research Fund. The costs of publication of this article were defrayed in part by the payment of page charges. This article must therefore be hereby marked "*advertisement*" in accordance with 18 U.S.C. Section 1734 solely to indicate this fact.

[1] To whom correspondence should be addressed. Tel.: 81-3-5363-3483; Fax: 81-3-5360-1508; E-mail: yoshimura@a6.keio.jp.

[2] The abbreviations used are: TLR, Toll-like receptor; RIG-I, retinoic acid-inducible gene-I; RLH, RIG-I-like helicase; IFN, interferon; IRF, interferon regulatory factor; NF-κB, nuclear factor κB; VSV, vesicular stomatitis virus; WT, wild type; MOI, multiplicity of infection; FBS, fetal bovine serum; LPS, lipopolysaccharide; DMEM, Dulbecco's modified Eagle's medium; BMDC, bone marrow-derived dendritic cells; GFP, green fluorescent protein; ELISA, enzyme-linked immunosorbent assay; JNK, c-Jun N-terminal kinase.

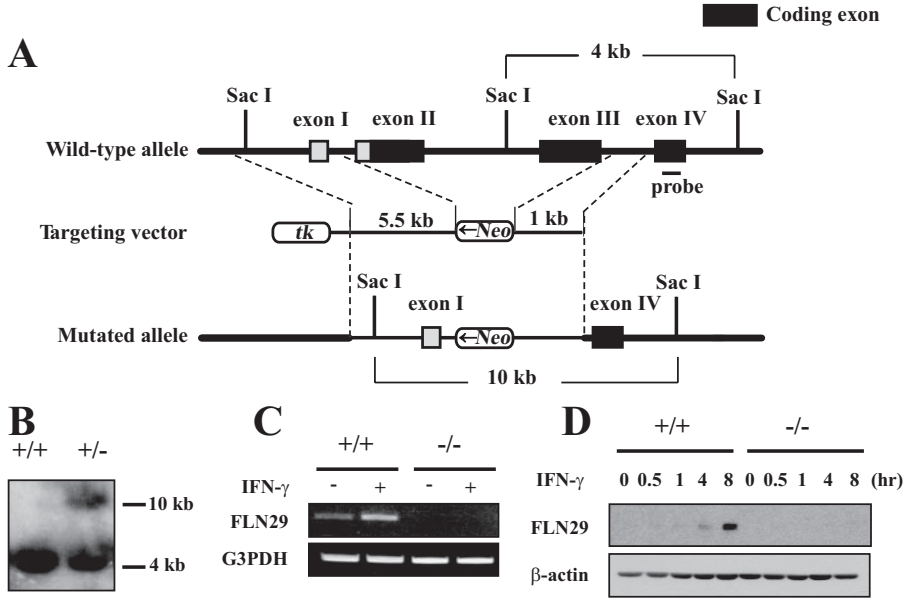

FIGURE 1. **Generation of FLN29-deficient mice.** *A*, schematic diagram of the mouse *FLN29* gene locus, the targeting vector, and the predicted targeted allele. *Open* and *closed boxes* denote the noncoding and coding exons, respectively. *B*, genomic DNA was extracted from ES cells, digested with SacI, electrophoresed, and hybridized with the indicated probe in *A*. The approximate size of the WT band is 4 kb, and the mutated band is 10 kb. *C* and *D*, BMDCs from WT and FLN29$^{-/-}$ mice were stimulated with 100 units/ml of IFN-γ for 6 h (*C*) or the indicated periods of time (*D*), and total RNA was then analyzed for *FLN29* by RT-PCR (*C*). Cell lysates were Western-blotted with anti-FLN29 antibody (*D*).

SHP-2, Cyld, and A20 have been reported as negative regulators of the RLH-IRF3 pathway (15–21). In our previous study, we demonstrated that FLN29 protein induced by type I or II IFNs acts as a negative regulator for the TLR4-TRAF6 signaling pathway in macrophages. FLN29 contains a TRAF-type zinc finger domain at its N terminus and a conserved TRAF6-binding motif at its middle portion. FLN29 interacts with the C terminus of TRAF6 through the TRAF6-binding motif, and inhibits TLR-dependent NF-κB and MAPK activation (22). Yet the physiological role of FLN29 remains unclear.

In this study, we generated FLN29-deficient (FLN29$^{-/-}$) mice and analyzed their TLR-dependent and RLH-dependent innate immune responses. We show here that FLN29$^{-/-}$ mice are indeed more susceptible to LPS-induced endotoxic shock. Furthermore, we have found a previously unidentified role for FLN29 in the RIG-I/IRF3 pathway. The present results show that FLN29 is a physiological negative regulator of TLR- and RLH-mediated innate immune responses.

EXPERIMENTAL PROCEDURES

Reagents and Antibodies—LPS from *Escherichia coli* (O111: B4), poly(I:C) and anti-FLAG (M2) antibody were purchased from Sigma-Aldrich. IFN-γ was purchased from Peprotech (London, UK). Anti-JNK1/2 (JNK) (cat. no. 9252), anti-phospho-IκBα (cat. no. 9246), anti-IκBα (cat. no. 9242) antibodies were from Cell Signaling Technology (Danvers, MA). Anti-phospho-JNK1/2 (cat. no. 612541) antibody was purchased from BD Transduction Laboratories (Franklin Lakes, NJ). Anti-T7 antibody (cat. no. 69522) was purchased from Novagen (Merck, Darmstadt, Germany). The expression vectors for T7-IPS-1 and IFN-β luciferase reporter plasmid have been described elsewhere (5). The expression vectors for FLAG-TRAF, 3×FLAG-TBK1, 3×FLAG-TANK, 3×FLAG-IRF3, and NF-κB luciferase reporter plasmid have been described in a previous report (22).

FLN29 Targeting Construct and Genotyping—The targeting vector was constructed by replacing the second and third exons with a PGK-*neo* cassette while preserving 5.5-kb (left arm) and 1-kb (right arm) flanks of homologous sequences. The HSV-*tk* gene was inserted for negative selection. Homologous recombination in murine 129/Sv ES cells was performed as described previously (23), and was confirmed by Southern blot analysis. The chimeric mice were backcrossed to C57BL/6J four times. The resultant heterozygous F4 mice were intercrossed to obtain the offspring used in our analyses. All experiments using these mice were approved by and performed according to the guidelines of the animal ethics committee of Kyushu University, Fukuoka, Japan.

Cell Culture—Primary WT and FLN29$^{-/-}$ mouse embryonic fibroblasts (MEFs) were prepared from E13.5 embryos and cultured in Dulbecco's modified Eagle's medium (DMEM) (Sigma) supplemented with 10% fetal bovine serum (FBS) (Biological Industries, Beit Haemek, Israel), penicillin/streptomycin (Nacalai Tesque, Kyoto, Japan), and L-glutamine (Nacalai Tesque). Primary MEFs were used at passages 3 and 4. Similar data were obtained in experiments using independently isolated MEFs. Bone marrow-derived dendritic cells (BMDCs) were generated as follows. Bone marrow cells from the femurs and tibiae of mice were cultured in RPMI1640 (Sigma) with 10% FBS, penicillin, streptomycin, and glutamine containing the culture supernatant from a J558L cell line transfected with the murine GM-CSF cDNA for 7 days, with replenishment of the medium every other day.

RT-PCR Analysis—Total RNA from MEFs, BMDCs, and HEK293T cells was extracted with RNAiso Plus (TaKaRa, Otsu, Japan) according to the manufacturer's instructions. Total RNA (1 μg) was reverse-transcribed using the Reverse Transcription kit (Applied BioSystems, Foster City, CA) with random hexamer. PCR analysis was performed using KOD Plus (TOYOBO, Osaka, Japan). The following oligonucleotides were used for PCR:G3PDH: (5′-ACCACAGTCCATGCCATCAC-3′ and 5′-TCCACCACCCTGTTGCTGTA-3′), IFN-β: (5′-TCCAAGAAAGGACGAACATTCG-3′ and 5′-TGAGGACATCTCCCACGTCCA-3′), IL-6: (5′-CCTCTCTGCAAGAGACTTCC-3′ and 5′-ACTCCTTCTGTGACTCCAGC-3′), IPS-1: (5′-ATGGCCCAGAGGAGAATGAGTATAAGTCCG-3′ and 5′-CTAGTGCAGACGCCGCCGGT-3′), and FLN29: (5′-ATGGCCGAGTTTCGAGATG-3′ and 5′-TCGATTTGTCTGAGGAGCTGGGA-3′).

Transfection and Reporter Assay—HEK293T cells (1.5×10^5/well) were seeded onto 6-well plates, and transfected using polyethylenimine (PEI, MW 25 kDa (Polysciences Inc., Warrington, PA)) in a 3:1 ratio to the amount of DNA. MEFs (1.0×10^5/well) were seeded into 6-well plates and transfected using FuGENE HD (Roche, Basel, Switzerland). The total concentration of transfected DNA was kept constant by supplementation with empty vector DNA. Luciferase activity was determined using the luciferase assay system (Promega, Madison, WI). The β-galactosidase vector was used for normalizing transfection efficiencies.

ELISA—The amounts of TNF-α, IL-6, and IL-12p70 were measured with OptEIA ELISA sets (BD Biosciences, Franklin Lakes, NJ) according to the manufacturer's instructions.

VSV Infection and Cytopathic Effect Assay—VSV has been previously described (24). 5.0×10^4 MEFs are seeded per well in 48-well plates, and then infected for 1.5 h with 5-fold serially diluted virus (from 0.02 MOI to 2.5 MOI). The cells were washed twice and replenished with 0.5% FBS-containing DMEM. After 36 h, the cytopathic effect was evaluated by staining with 0.5% (w/v) crystal violet. Cell viability was examined using the Cell Count Reagent SF kit (Nacalai Tesque). VSVΔG-EGFP was prepared as described (25).

Plaque Assay—Culture supernatants were collected from MEFs infected with VSV. Virus yield in culture supernatants was determined by standard plaque assay using Vero cells. Vero cells were infected with serially diluted culture supernatants. After incubation for 2 h, the infected cells were washed twice with DMEM containing 0.5% FBS and overlaid with DMEM containing 2% methyl cellulose and 2% FBS. After 36 h of incubation, the number of plaques was counted.

Immunoprecipitation and Western Blotting—Cells were washed twice with ice-cold phosphate-buffered saline and lysed in 0.1 ml of 10 mM Tris-HCl, pH 7.4, 150 mM NaCl, 0.5 mM EDTA, 1% Nonidet P-40, 10 mM NaF, 1 mM dithiothreitol, 1 mM sodium orthovanadate, and 1 mM phenylmethylsulfonyl fluoride supplemented with protease inhibitor mixture (Nacalai Tesque). Cellular debris was removed by centrifugation at $15{,}000 \times g$ for 30 min. Proteins from cell lysates were immunoprecipitated with 1 μg of antibody and 15 μl of protein G-Sepharose (GE Healthcare, Chalfont St. Giles, Bucks, UK) for 1.5 h at 4 °C. The immune complex was washed five times with washing buffer containing 50 mM Tris-HCl, pH 7.4, 150 mM NaCl, and 0.5% Triton X-100. For Western blotting, the immunoprecipitates or total cell lysates were resolved on SDS-polyacrylamide gel electrophoresis (SDS-PAGE) and transferred onto Immobilon-P PVDF membranes (Millipore, Billerica, MA). The membranes were incubated with various primary antibodies, and the bound antibodies were visualized with horseradish peroxidase-conjugated antibodies against rabbit or mouse IgG using Chemi-Lumi One L Western blotting detection reagents (Nacalai Tesque).

Native PAGE—Non-SDS-polyacrylamide gel (7.5%) was prerun with 25 mM Tris-HCl and 192 mM glycine, pH 8.4 with and without 0.2% deoxycholate in the cathode and anode chamber, respectively, for 30 min at 40 mA. Samples in the native sample buffer (10 μg of protein, 62.5 mM Tris-Cl, pH 6.8, 15% glycerol) were applied to the gel and electrophoresed at 25 mA for 50 min.

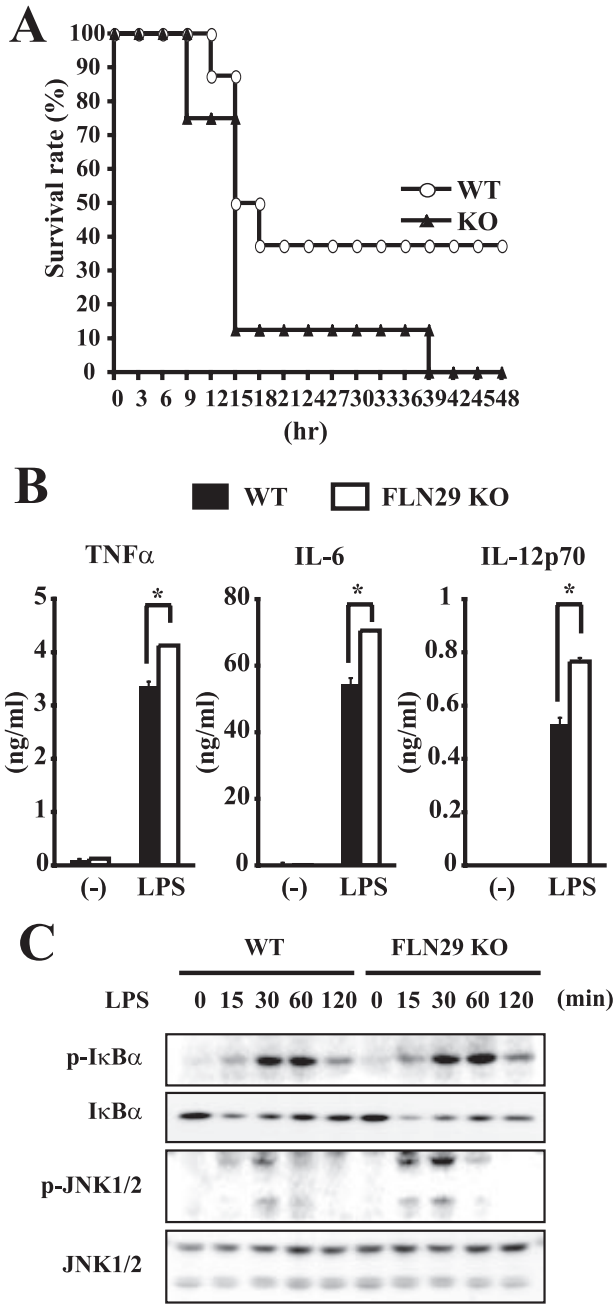

FIGURE 2. **FLN29 deficiency exhibits enhanced response to LPS *in vivo* and *in vitro*.** *A*, 8-week-old WT ($n = 8$) and FLN29$^{-/-}$ ($n = 8$) mice were intraperitoneally injected with LPS (18 μg/g), and survival was monitored for the following 48 h. *B*, BMDCs from WT and FLN29$^{-/-}$ mice were stimulated with LPS (10 ng/ml). After 6 h, the levels of TNFα, IL-6, and IL-12p70 in the culture supernatants were determined by ELISA. Values are means ± S.D. from triplicate cultures in three independent experiments. *, $p < 0.003$. *C*, BMDCs from WT and FLN29$^{-/-}$ mice were stimulated with LPS (10 ng/ml) for the indicated periods of time, and cell lysates were analyzed by Western blotting with anti-phospho-IκBα, anti-IκBα, anti-phospho-JNK1/2, and anti-JNK1/2 antibodies.

RESULTS

Generation of FLN29-deficient Mice—To assess the physiological role of FLN29, we generated mice lacking the *FLN29* gene (Fig. 1). FLN29$^{-/-}$ mice were born at the expected Men-

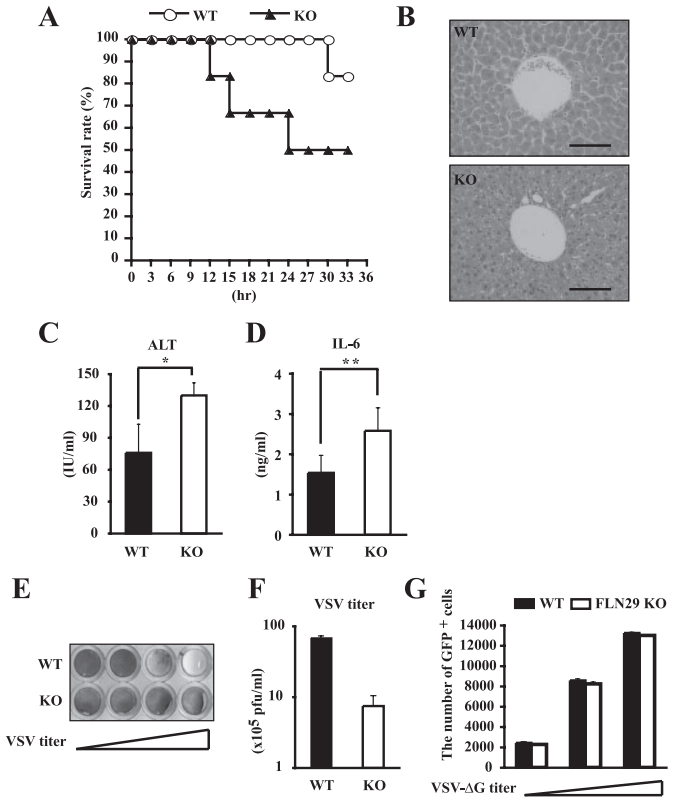

FIGURE 3. **FLN29 also functions as a negative regulator of the RLH pathway.** *A*, 8-week-old WT ($n = 6$) and FLN29$^{-/-}$ ($n = 6$) mice were intraperitoneally injected with poly(I:C) plus D-Gal N (20 μg plus 20 mg/body), and survival was monitored for the following 36 h. *B*, histological examination of the livers of WT and FLN29$^{-/-}$ mice at 6 h after poly(I:C) and D-Gal N injection. H&E staining is shown. *Scale bars*, 100 μm. *C* and *D*, serum ALT (*C*) and IL-6 levels (*D*) were analyzed. Sera were taken at 6 h (*C*) or 2 h (*D*) after poly(I:C) plus D-Gal N injection ($n = 3$). Values are means ± S.D. from three independent experiments. *, $p < 0.035$; **, $p < 0.012$. *E*, MEFs from WT and FLN29$^{-/-}$ mice were infected with VSV (MOI = 0.02, 0.1, 0.5, and 2.5). The viral cytopathic effect at 36 h was visualized by crystal violet staining. *F*, virus titers in the culture supernatants 36 h after VSV infection (0.5 MOI) were determined by plaque assay. *G*, MEFs from WT and FLN29$^{-/-}$ mice were infected with VSVΔG-EGFP (MOI = 0.125, 0.25, and 0.5). 12 h later, the number of GFP-positive cells was counted by FACS analysis. Indicated values are means ± S.D. of triplicate samples.

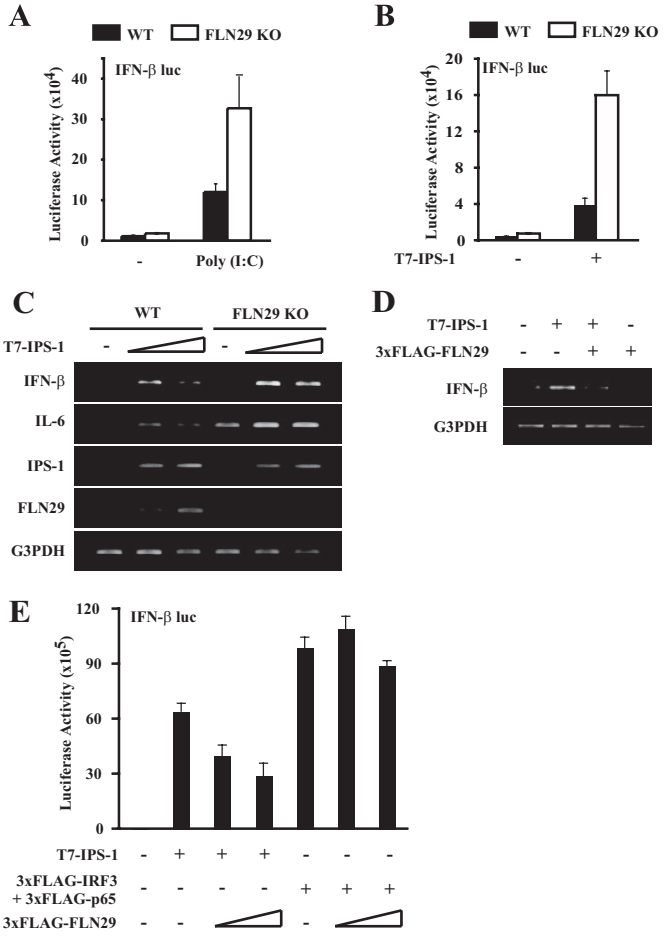

FIGURE 4. **FLN29 inhibits RLH-dependent IFN-β induction.** *A*, WT and FLN29$^{-/-}$ MEFs were transiently transfected with the IFN-β promoter and β-galactosidase reporter plasmids, and stimulated with poly(I:C) plus FuGENE HD. Luciferase activity was measured at 12 h after poly(I:C) transfection and normalized based on β-galactosidase levels. *B*, WT and FLN29$^{-/-}$ MEFs were transiently transfected with the IFN-β promoter and β-galactosidase reporter plasmids in the presence (+) or absence (−) of IPS-1 expression plasmid. Luciferase activity was measured 36 h after transfection. *C*, WT and FLN29$^{-/-}$ MEFs cells were transiently transfected with the expression plasmid for T7-IPS-1 (0.5 and 1 μg/well). Total RNA was prepared 28 h after transfection and was analyzed by RT-PCR for the expression of *IFN-β*, *IL-6*, *IPS-1*, *FLN29*, and *G3PDH*. *D*, HEK293T cells were transiently transfected with the indicated combination of expression plasmids. Total RNA was prepared at 24 h after transfection and was analyzed by RT-PCR for the expression of *IFN-β* and *G3PDH*. *E*, HEK293T cells were transiently transfected with the indicated combination of expression plasmids for T7-IPS-1, 3×FLAG-FLN29 (0.2 and 0.5 μg/well), 3×FLAG-IRF3, and 3×FLAG-p65 along with the IFN-β promoter and β-galactosidase reporter plasmids. Luciferase activity was measured at 36 h after transfection.

delian ratio with no gross developmental abnormalities (data not shown). We confirmed the absence of FLN29 at the genomic, mRNA, and protein levels (Fig. 1, *B–D*). The expression of mRNA and protein of FLN29 was induced upon IFN-γ stimulation in BMDCs from WT mice, but not from FLN29$^{-/-}$ mice (Fig. 1, *C* and *D*). A basal level expression of FLN29 was readily detectable by RT-PCR in WT BMDCs (Fig. 1*C*).

FLN29 Deficiency Leads to Enhanced Response to LPS in Vivo and in Vitro—Our previous *in vitro* study has suggested that FLN29 negatively regulates TLR4 signaling (22). Therefore, we first tested the effect of FLN29 deficiency on LPS response *in vivo* by injecting a sublethal dose of LPS into WT and FLN29$^{-/-}$ mice. We found that FLN29$^{-/-}$ mice were more sensitive to LPS-induced septic shock than WT mice (Fig. 2*A*). We then analyzed production of pro-inflammatory cytokines such as IL-6, TNFα, and IL-12 p70 by BMDCs upon stimulation with LPS *in vitro*. As shown in Fig. 2*B*, the levels of these pro-inflammatory cytokines were enhanced in FLN29$^{-/-}$ BMDCs compared with WT BMDCs. Furthermore, the LPS-induced activation of IKK and that of JNK1/2 were elevated in FLN29$^{-/-}$ BMDCs compared with WT (Fig. 2*C*). These results, which are consistent with our previous findings (22), define the physiological role of FLN29 as a negative regulator of TLR4 signaling.

FLN29 Also Functions as a Negative Regulator of the RLH Pathway—It has recently been shown that TRAF6 also mediates RLH-dependent signaling (8)[3]. In response to this discovery, we next attempted to determine whether FLN29 might also regulate the RLH signaling pathways, by challenging mice with poly(I:C), a synthetic dsRNA which stimulates both TLR3 and RLH pathways *in vivo*. As shown in Fig. 3*A*, FLN29$^{-/-}$ mice

[3] R. Yoshida, unpublished results.

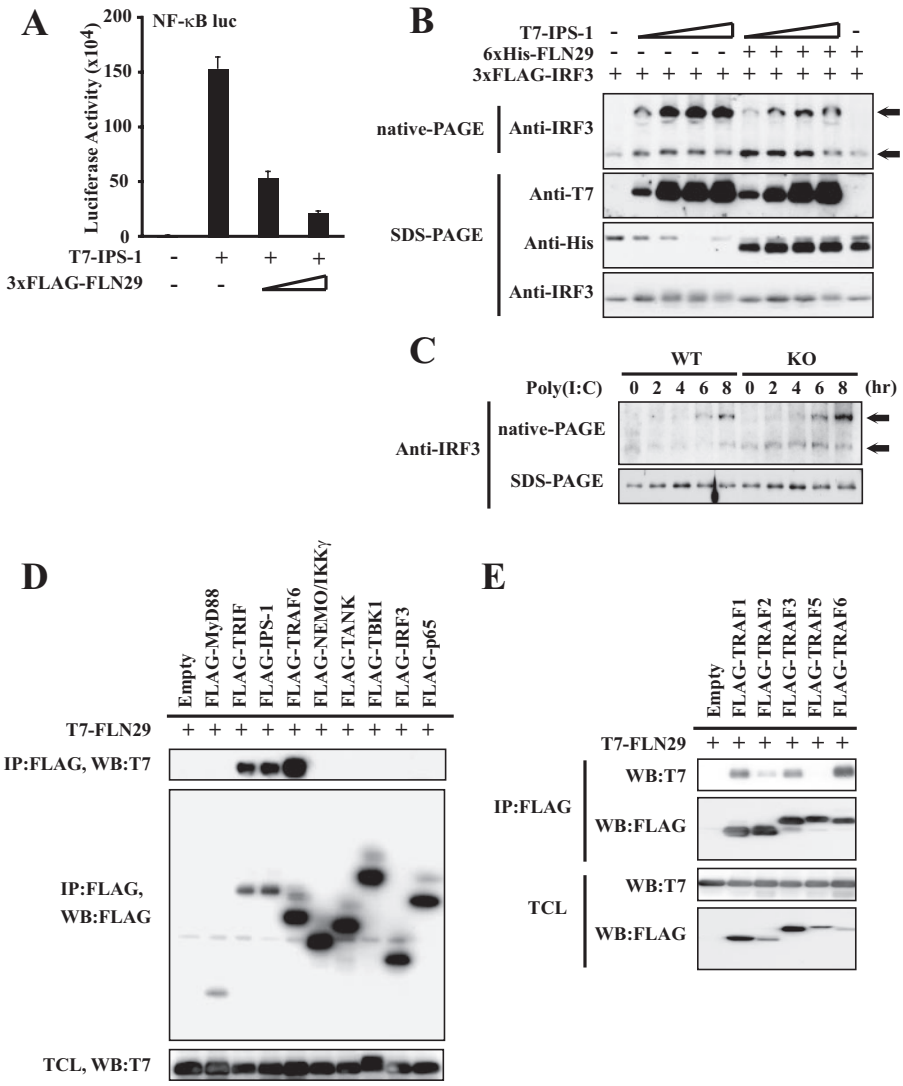

FIGURE 5. **FLN29 inhibits IPS-1-dependent NF-κB and IRF3 activation.** *A*, HEK293T cells were transiently transfected with the indicated combination of T7-IPS-1 and 3×FLAG-FLN29 (0.2 and 0.5 μg/well) expression plasmids along with the NF-κB reporter and β-galactosidase expression plasmids. Luciferase activity was measured at 36 h after transfection. *B*, HEK293T cells were transiently transfected with the combinations of 3×FLAG-IRF3, T7-IPS-1 (0.01, 0.05, 0.1, and 0.2 μg/well), and 6×His-FLN29 as indicated. Cell lysates were separated by native PAGE or SDS-PAGE followed by Western blotting with the indicated antibodies. *Upper* and *lower arrows* indicate dimeric and monomeric form of IRF3, respectively. *C*, WT and FLN29$^{-/-}$ MEFs were stimulated with poly(I:C) plus FuGENE HD. Cell lysates were separated by native PAGE or SDS-PAGE followed by Western blotting with anti-IRF3 antibody. *Upper* and *lower arrows* indicate dimeric and monomeric form of IRF3, respectively. *D* and *E*, HEK293T cells were transiently transfected with T7-FLN29 together with the indicated expression plasmids, and cell extracts were immunoprecipitated (*IP*) with anti-FLAG antibody. The immunoprecipitates and total cell lysates (*TCL*) were separated by SDS-PAGE and Western-blotted (*WB*) with the indicated antibodies.

were significantly more sensitive to poly(I:C)-induced shock than WT mice. Histological analysis and serum ALT levels demonstrated that FLN29$^{-/-}$ mice suffered more severe hepatic damage than WT mice (Fig. 3, *B* and *C*). Serum IL-6 level at 2 h after poly(I:C) injection was also elevated in FLN29$^{-/-}$ mice (Fig. 3*D*). These results indicate that FLN29 may negatively regulate either the TLR3 or the RLH signaling pathway, or both.

To determine whether the RLH pathway is targeted by FLN29, we examined the antiviral response of MEFs against VSV. We found that FLN29$^{-/-}$ MEFs were more resistant to VSV-induced cytopathic effect (Fig. 3*E*). The virus titer in the culture supernatant collected at 36 h after infection was significantly lower in FLN29$^{-/-}$ MEFs than in WT (Fig. 3*F*). To exclude the possibility that *FLN29* deficiency simply reduces the efficiency of primary infection, we tested the infectivity of VSVΔG-EGFP. VSVΔG-EGFP is a recombinant VSV that is incapable of secondary infection due to the replacement of the viral G protein gene with the *GFP* gene (25). No difference was observed between WT and FLN29$^{-/-}$ MEFs in the infectivity of VSVΔG-EGFP (Fig. 3*G*). Thus, FLN29 deficiency results in resistance to VSV multiplication without affecting the efficiency of primary infection. Together, these data indicate that FLN29 plays a negative regulatory role in the RLH-mediated signaling pathway.

FLN29 Inhibits RLH-dependent IFN-β Induction—The above results prompted us to ask whether *FLN29* deficiency could augment RLH-dependent type I IFN production. So, we tested the effect of *FLN29* deficiency on poly(I:C)- or IPS-1-induced IFN-β promoter activity. As shown in Fig. 4, *A* and *B*, *FLN29* deficiency enhanced poly(I:C)- or IPS-1-induced IFN-β promoter activation. The expression of endogenous IFN-β and IL-6 induced by IPS-1 was also elevated in FLN29$^{-/-}$ MEFs compared with WT cells (Fig. 4*C*). Conversely, overexpression of FLN29 inhibited the IPS-1-induced expression of endogenous IFN-β (Fig. 4*D*). Similar results were obtained by reporter assay using the IFN-β promoter, while FLN29 had no inhibitory effect on the activation of IFN-β promoter by co-expression of the p65 subunit of NF-κB and IRF3 (Fig. 4*E*). Therefore, it is likely that FLN29 negatively regulates the RLH pathway downstream of IPS-1 and upstream of NF-κB and IRF3.

FLN29 Inhibits IPS-1-dependent NF-κB and IRF3 Activation at the Level of the IPS-1/TRAF Protein Complex—RLH-IPS-1 signaling bifurcates into the NF-κB pathway and the IRF3 pathway (1). To further investigate the mechanism by which FLN29 suppresses the RLH signaling pathway, we examined the effect of FLN29 overexpression on the activation of NF-κB and IRF3, both of which have been shown to be essential transcription factors for IFN-β production by the RLH-IPS-1 pathway (9, 10). As shown in Fig. 5*A*, overexpression of FLN29 inhibited the

activation of NF-κB induced by IPS-1. Overexpression of FLN29 also inhibited IPS-1-dependent IRF3 activation, as assessed by dimer formation of IRF3 in native PAGE (Fig. 5*B*). On the contrary, FLN29$^{-/-}$ MEFs showed an elevated level of IRF3 dimerization upon poly(I:C) transfection compared with WT MEFs (Fig. 5*C*). These results indicate that FLN29 negatively regulates both the NF-κB pathway and the IRF3 pathway. To gain insight into the molecular mechanism by which FLN29 inhibits RLH-IPS-1 signaling, we examined the complex formation of FLN29 with other molecules involved in either the RLH or TLR pathway. In addition to its binding to TRAF6, we found that FLN29 interacts with IPS-1, TRIF, TRAF1, -2, and -3 (Fig. 5, *D* and *E*). These results imply that FLN29 acts at the level of the IPS-1/TRAF protein complex, where it suppresses both NF-κB and IRF3.

DISCUSSION

In this study, we generated FLN29$^{-/-}$ mice to discern the physiological role of FLN29. As expected from our previous work (22), FLN29$^{-/-}$ mice exhibited increased susceptibility to LPS-induced endotoxic shock with increased production of pro-inflammatory cytokines, thereby demonstrating the negative regulatory role of FLN29 in *in vivo* TLR4 signaling. In addition, the analysis of FLN29$^{-/-}$ mice led us to identify a previously unknown function of FLN29 as a negative regulator of the RLH signaling pathway. We found that FLN29$^{-/-}$ MEFs were more resistant to VSV infection and that these cells produced more IFN-β upon activation of the RLH pathway. Conversely, overexpression of FLN29 inhibited IPS-1-dependent induction of IFN-β. Together, the results of our study provide the first genetic evidence supporting the negative regulatory role of FLN29 in the TLR and RLH signaling pathways.

Negative regulatory molecules can play one of three types of physiological roles. In the first possible scenario, the negative regulator keeps the effector molecule inactive in resting cells. In the second, the negative regulator influences the strength of the signal to maintain the entire response at an appropriate level. In the third, the negative regulator terminates the response. *FLN29* deficiency by itself did not result in the activation of the signaling pathway, nor in the prolonged activation of the pathway, but rather in the augmented activation of IKK and JNK (Fig. 2*C*), indicating that FLN29 may contribute to a fine-tuning mechanism regulating innate immune responses.

It is currently unclear exactly how FLN29 regulates the TLR and RLH signaling pathways. As FLN29 is capable of binding to IPS-1, TRAF3, and TRAF6 (Fig. 5, *D* and *E*), it is likely that FLN29 might target the multiprotein complex composed of these molecules. Recent studies have identified negative regulatory proteins such as A20, CYLD, and DUBA, all of which possess deubiquitination activity (DUB) toward several signaling molecules, including RIG-I, TRAF3, and TRAF6 (17–21). FLN29 protein, however, does not contain a DUB domain and therefore is unlikely to function as a DUB. We speculate, rather, that FLN29 might interfere with the complex formation process of IPS-1 and TRAF proteins in the RLH pathway, thereby inhibiting the activation of both NF-κB and IRF3. It has recently been reported that TRADD is critically involved in the RLH-dependent induction of IFN-β (26). TRADD forms a multiprotein complex with Cardif (IPS-1), TRAF3, TANK, FADD, and RIP1, leading to the activation of both NF-κB and IRF3. It is also possible that FLN29 might act on TRADD to inhibit the assembly of this signaling complex. Further study is needed to elucidate the molecular mechanisms of FLN29 action in detail.

FLN29 interacts physically with several TRAF family proteins including TRAF1, -2, -3, and -6 (Fig. 5*E*). Because TRAF proteins are involved in a wide variety of signaling pathways, not only downstream of TLRs but also downstream of TNF family receptors, it is important to determine whether FLN29, too, might regulate such signaling pathways. Our preliminary data show that FLN29$^{-/-}$ BMDCs also produce a higher level of TNFα and IL-6 in response to CpG DNA (data not shown), indicating that FLN29 may be involved in TLR9 signaling as well. The question of whether FLN29 has any role in the regulation of TNF family receptor signaling, such as TNFR, RANK, or CD40, awaits further investigation.

We have demonstrated that FLN29$^{-/-}$ mice exhibit enhanced induction of inflammatory cytokines and higher susceptibility to LPS- and poly(I:C)-induced endotoxic shock. TLR-mediated activation of innate immunity, when in excess, triggers development of autoimmune disorders, and inflammatory diseases, such as systemic lupus erythematosus, cardiomyopathy, atherosclerosis, diabetes mellitus, and inflammatory bowel diseases. Because dysregulation of type I or type II IFNs and of inflammatory cytokine production drives these diseases, FLN29 might be involved in the disease process. Future studies with the animal models of these diseases in FLN29$^{-/-}$ mice will enhance our knowledge of the general pathogenesis of these diseases.

Acknowledgments—We thank N. Kinoshita, M. Ohtsu, and Y. Yamada (Technical Support Center, Medical Institute of Bioregulation) and T. Yoshioka for technical support and Y. Nishi for preparing the manuscript. We thank Dr. Y. Yanagi (Kyushu University) for VSVΔG-EGFP system and Dr. K. Kuroda (Nihon University) and Dr. S. Nagafuchi (Kyushu University) for virus experiments.

REFERENCES

1. Takeuchi, O., and Akira, S. (2007) *Immunol. Rev.* **220,** 214–224
2. Akira, S., and Takeda, K. (2004) *Nat. Rev. Immunol.* **4,** 499–511
3. Gitlin, L., Barchet, W., Gilfillan, S., Cella, M., Beutler, B., Flavell, R. A., Diamond, M. S., and Colonna, M. (2006) *Proc. Natl. Acad. Sci. U. S. A.* **103,** 8459–8464
4. Yoneyama, M., Kikuchi, M., Natsukawa, T., Shinobu, N., Imaizumi, T., Miyagishi, M., Taira, K., Akira, S., and Fujita, T. (2004) *Nat. Immunol.* **5,** 730–737
5. Kawai, T., Takahashi, K., Sato, S., Coban, C., Kumar, H., Kato, H., Ishii, K. J., Takeuchi, O., and Akira, S. (2005) *Nat. Immunol.* **6,** 981–988
6. Meylan, E., Curran, J., Hofmann, K., Moradpour, D., Binder, M., Bartenschlager, R., and Tschopp, J. (2005) *Nature* **437,** 1167–1172
7. Seth, R. B., Sun, L., Ea, C. K., and Chen, Z. J. (2005) *Cell* **122,** 669–682
8. Xu, L. G., Wang, Y. Y., Han, K. J., Li, L. Y., Zhai, Z., and Shu, H. B. (2005) *Mol. Cell* **19,** 727–740
9. Lenardo, M. J., Fan, C. M., Maniatis, T., and Baltimore, D. (1989) *Cell* **57,** 287–294
10. Sato, M., Suemori, H., Hata, N., Asagiri, M., Ogasawara, K., Nakao, K., Nakaya, T., Katsuki, M., Noguchi, S., Tanaka, N., and Taniguchi, T. (2000) *Immunity* **13,** 539–548
11. Yoshimura, A., Naka, T., and Kubo, M. (2007) *Nat. Rev. Immunol.* **7,** 454–465

12. Boone, D. L., Turer, E. E., Lee, E. G., Ahmad, R. C., Wheeler, M. T., Tsui, C., Hurley, P., Chien, M., Chai, S., Hitotsumatsu, O., McNally, E., Pickart, C., and Ma, A. (2004) *Nat. Immunol.* **5,** 1052–1060
13. Kinjyo, I., Hanada, T., Inagaki-Ohara, K., Mori, H., Aki, D., Ohishi, M., Yoshida, H., Kubo, M., and Yoshimura, A. (2002) *Immunity* **17,** 583–591
14. Kobayashi, K., Hernandez, L. D., Galan, J. E., Janeway, C. A., Jr., Medzhitov, R., and Flavell, R. A. (2002) *Cell* **110,** 191–202
15. An, H., Zhao, W., Hou, J., Zhang, Y., Xie, Y., Zheng, Y., Xu, H., Qian, C., Zhou, J., Yu, Y., Liu, S., Feng, G., and Cao, X. (2006) *Immunity* **25,** 919–928
16. Arimoto, K., Takahashi, H., Hishiki, T., Konishi, H., Fujita, T., and Shimotohno, K. (2007) *Proc. Natl. Acad. Sci. U. S. A.* **104,** 7500–7505
17. Friedman, C. S., O'Donnell, M. A., Legarda-Addison, D., Ng, A., Cardenas, W. B., Yount, J. S., Moran, T. M., Basler, C. F., Komuro, A., Horvath, C. M., Xavier, R., and Ting, A. T. (2008) *EMBO Rep.* **9,** 930–936
18. Kayagaki, N., Phung, Q., Chan, S., Chaudhari, R., Quan, C., O'Rourke, K. M., Eby, M., Pietras, E., Cheng, G., Bazan, J. F., Zhang, Z., Arnott, D., and Dixit, V. M. (2007) *Science* **318,** 1628–1632
19. Lin, R., Yang, L., Nakhaei, P., Sun, Q., Sharif-Askari, E., Julkunen, I., and Hiscott, J. (2006) *J. Biol. Chem.* **281,** 2095–2103
20. Saitoh, T., Yamamoto, M., Miyagishi, M., Taira, K., Nakanishi, M., Fujita, T., Akira, S., Yamamoto, N., and Yamaoka, S. (2005) *J. Immunol.* **174,** 1507–1512
21. Zhang, M., Wu, X., Lee, A. J., Jin, W., Chang, M., Wright, A., Imaizumi, T., and Sun, S. C. (2008) *J. Biol. Chem.* **283,** 18621–18626
22. Mashima, R., Saeki, K., Aki, D., Minoda, Y., Takaki, H., Sanada, T., Kobayashi, T., Aburatani, H., Yamanashi, Y., and Yoshimura, A. (2005) *J. Biol. Chem.* **280,** 41289–41297
23. Taniguchi, K., Ayada, T., Ichiyama, K., Kohno, R., Yonemitsu, Y., Minami, Y., Kikuchi, A., Maehara, Y., and Yoshimura, A. (2007) *Biochem. Biophys. Res. Commun.* **352,** 896–902
24. Sakamoto, H., Yasukawa, H., Masuhara, M., Tanimura, S., Sasaki, A., Yuge, K., Ohtsubo, M., Ohtsuka, A., Fujita, T., Ohta, T., Furukawa, Y., Iwase, S., Yamada, H., and Yoshimura, A. (1998) *Blood* **92,** 1668–1676
25. Takada, A., Robison, C., Goto, H., Sanchez, A., Murti, K. G., Whitt, M. A., and Kawaoka, Y. (1997) *Proc. Natl. Acad. Sci. U. S. A.* **94,** 14764–14769
26. Michallet, M. C., Meylan, E., Ermolaeva, M. A., Vazquez, J., Rebsamen, M., Curran, J., Poeck, H., Bscheider, M., Hartmann, G., Konig, M., Kalinke, U., Pasparakis, M., and Tschopp, J. (2008) *Immunity* **28,** 651–661